ARTICLE

Micropatterning of Proteins and Mammalian Cells on Indium Tin Oxide

Sunny S. Shah,[†] Michael C. Howland,[†] Li-Jung Chen,[#] Jaime Silangcruz,[†] Stanislav V. Verkhoturov,[#] Emile A. Schweikert,[#] Atul N. Parikh,[§,⊥] and Alexander Revzin*[,†]

Department of Biomedical Engineering, Department of Chemical Engineering and Materials Science, Department of Biophysics, and Applied Science Graduate Group, University of California, Davis, California 95616, and Department of Chemistry, Texas A&M University, College Station, Texas 77843

ABSTRACT This paper describes a novel surface engineering approach that combines oxygen plasma treatment and electrochemical activation to create micropatterned cocultures on indium tin oxide (ITO) substrates. In this approach, photoresist was patterned onto an ITO substrate modified with poly(ethylene) glycol (PEG) silane. The photoresist served as a stencil during exposure of the surface to oxygen plasma. Upon incubation with collagen (I) solution and removal of the photoresist, the ITO substrate contained collagen regions surrounded by nonfouling PEG silane. Chemical analysis carried out with time-of-flight secondary ion mass spectrometry (ToF-SIMS) at different stages in micropatterned construction verified removal of PEG-silane during oxygen plasma and presence of collagen and PEG molecules on the same surface. Imaging ellipsometry and atomic force microscopy (AFM) were employed to further investigate micropatterned ITO surfaces. Biological application of this micropatterning strategy was demonstrated through selective attachment of mammalian cells on the ITO substrate. Importantly, after seeding the first cell type, the ITO surfaces could be activated by applying negative voltage (−1.4 V vs Ag/AgCl). This resulted in removal of nonfouling PEG layer and allowed to attach another cell type onto the same surface and to create micropatterned cocultures. Micropatterned cocultures of primary hepatocytes and fibroblasts created by this strategy remained functional after 9 days as verified by analysis of hepatic albumin. The novel surface engineering strategy described here may be used to pattern multiple cell types on an optically transparent and conductive substrate and is envisioned to have applications in tissue engineering and biosensing.

KEYWORDS: indium tin oxide • photolithography • switchable surfaces • protein micropatterning • cell micropatterning • imaging ellipsometry • microfabrication

INTRODUCTION

The ability to design cellular interactions is important for creating in vitro models that mimic complexity of native tissue (1–3). One approach employed frequently in biology is cultivating two cell types as a way to ensure that cell function is better maintained in a culture dish. Cultivation of two cell types, or coculture, is particularly important in liver tissue engineering where hepatocytes cocultured with supporting (nonparenchymal) cells maintain hepatic function longer and at a much higher level than hepatocytes cultured alone (4, 5).

Traditionally, cocultures were created by random seeding of the two cell types in a culture. In a series of seminal papers, Bhatia and colleagues proposed to employ surface micropatterning (photolithography) to define sites for attachment of hepatocytes and supporting cells, and showed improved hepatic function of such cell culture system (6–8). In this approach, photoresist was patterned on the glass surface and used as a stencil for adsorption of cell-adhesive protein molecules (collagen I). Construction of the coculture was based on preference of hepatocytes to attach to collagen and the ability of fibroblasts to adhere elsewhere on the surface (8). While offering outstanding insight into interactions between two cell types, this coculture micropatterning approach relied on cell type-specific adhesion preferences and therefore could not be easily translated to other cell types. A number of alternative micropatterning approaches have been developed to better control cell-surface interactions and to organize multiple cell types on the same surface. These approaches have utilized microfluidic channels (9, 10), polymer stencils (11, 12), layer-by-layer electrostatic interactions (13), stimuli-responsive polymers (14), and electrochemical activation (15, 16) to define the time and place of cell attachment.

Electrical stimulation is particularly appealing as a method for controlling composition of biointerface (17) and for guiding cell-surface interactions (15, 16, 18–23). This strategy requires minimal handling of the culture substrate; electrical stimulus can be applied in cell culture media so that the location and time of stimulation may be controlled precisely through the use of electrode arrays (21, 22, 24). The majority of electrochemical switching strategies have focused on altering properties of gold substrates modified

* To whom correspondence should be addressed. Mailing address: Department of Biomedical Engineering, University of California, Davis, 451 East Health Sciences St. #2619, Davis, CA, 95616. E-mail: arevzin@ucdavis.edu. Phone: 530-752-2383. Fax: 530-754-5739.

Received for review July 30, 2009 and accepted October 14, 2009

[†] Department of Biomedical Engineering, University of California.

[‡] Department of Chemical Engineering and Materials Science, University of California.

[#] Department of Chemistry, Texas A&M University.

[§] Department of Biophysics, University of California.

[⊥] Applied Science Graduate Group, University of California.

DOI: 10.1021/am900508m

© 2009 American Chemical Society

Published on Web 10/30/2009

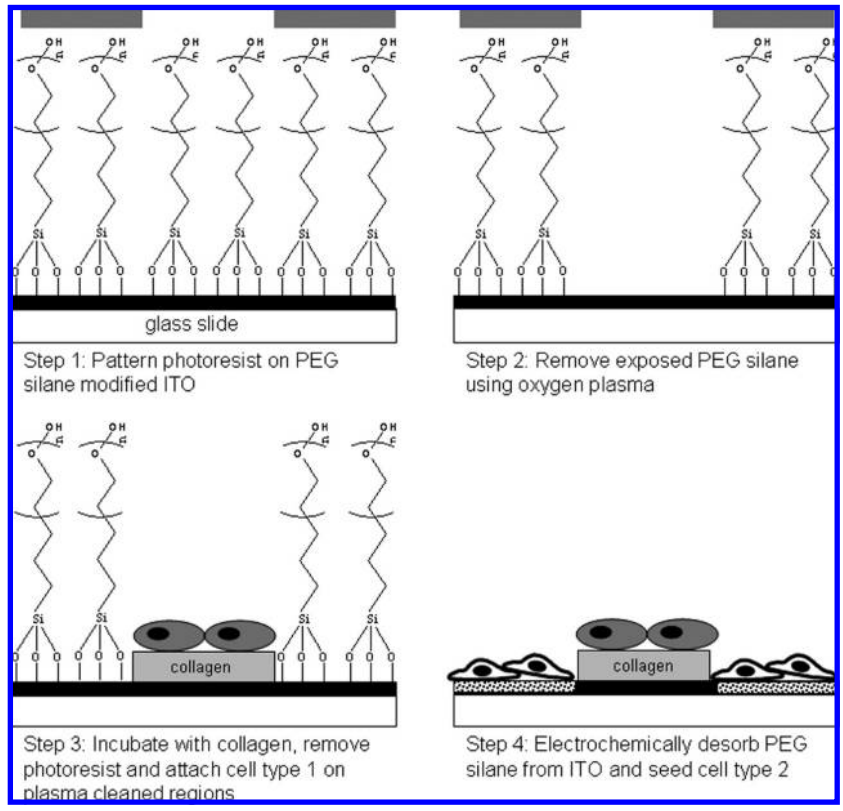

FIGURE 1. Novel surface engineering strategy for micropatterning one or two cell types on ITO. Step 1: ITO coated glass slides are modified with a nonfouling PEG silane. Photoresist is then patterned on top of PEG-modified ITO. Step 2: The substrate is exposed to oxygen plasma which removes PEG from regions of ITO not protected by photoresist. Step 3: The substrate is then incubated with cell-adhesive ligands (collagen I in our case) followed by photoresist liftoff. Upon incubation with the patterned ITO substrate, cells of type I selectively attach to the cell-adhesive domains to form micropatterns. Step 4: Applying reductive potential (−1.4 vs Ag/AgCl reference for 60 s) results in desorption of the remaining PEG silane. Electrical stimulation switches ITO surface properties and allows for attachment of cell type II to form a coculture.

with self-assembled monolayers (15, 17, 18). Gold is an excellent electrode material; however, it is not optically transparent and therefore is not optimal for cell cultivation. While gold can be semitransparent when deposited as a thin layer and may serve as a cell culture substrate (25), it will no longer function properly as an electrode because of increased resistivity. ITO, on the other hand, combines excellent conductivity with optical transparency and has been used in electrophysiology (26), cell cultivation (27), and cell-based biosensing (28). Electrochemical switching of ITO surface properties has been demonstrated in a few recent publications (21, 24, 29, 30).

Functionalization with poly(ethylene glycol) (PEG) renders surfaces resistive to adhesion of cells and proteins (31, 32). Previously, we demonstrated electrochemical desorption of a nonfouling PEG silane layer from ITO substrate as a way to exercise spatial and temporal control over cell attachment (21). Building on this prior work, the present paper sought to develop and characterize a simple and effective method for micropatterning cells in mono- and co-cultures on ITO. A novel micropatterning approach developed for this purpose involved patterning photoresist on nonfouling (PEG-silane modified) ITO substrate and then treating this substrate in oxygen plasma to selectively remove PEG silane from regions not protected by photoresist (see Figure 1). Immersion of this surface in a solution of cell-adhesive protein (e.g., collagen I) followed by photoresist lift-off resulted in a surface comprised of cell-adhesive collagen (I) islands within a layer of nonfouling PEG. Chemical and topographic analysis of these micropatterned substrates was performed at different stages in surface preparation using time-of-flight secondary ion mass spectrometry (ToF-SIMS), imaging ellipsometry (IE) and atomic force microscopy (AFM). To further develop biological application of this micropatterning strategy we demonstrated that primary rat hepatocytes attached selectively on regions of the ITO substrate containing matrix proteins and did not attach on PEG-modified regions. Applying reductive voltage (−1.4 V vs Ag/AgCl) to the ITO substrate containing hepatocytes led to desorption of the surrounding PEG-silane layer. A second cell type (fibroblasts) could now be added to the surface to complete the coculture. Importantly, hepatocytes were not affected by the electrical stimulation of the surface and remained functional on ITO.

MATERIALS AND METHODS

Chemicals and Materials. Indium Tin Oxide (ITO) coated glass slides (75 × 25 mm) were obtained from Delta Technologies (Stillwater, MN). The ITO coated glass slides had sheet resistance of 4−8 Ω with nominal transmittance of >82% and an ITO thickness of 150−200 nm. 2-[Methoxy(polyethylenoxy)propyl] trichlorosilane (MW range 470−610) (PEG silane) was purchased from Gelest, Inc. Ethanol, acetone, anhydrous tolu-

ene, and collagen from rat tail (type I) were purchased from Sigma-Aldrich (St. Louis, MO). Phosphate-buffered saline (PBS) 10X was purchased from Cambrex. Dulbecco's modified Eagles' medium (DMEM), Minimal Essential Medium (MEM), sodium pyruvate, nonessential amino acids, fetal bovine serum (FBS), FITC-labeled collagen type I were purchased from Invitrogen Life Technologies (Carlsbad, CA). The 384-well polypropylene microarray plates were obtained from Genetix (New Milton, NH). Goat antirat albumin antibody, goat antirat albumin antibody-HRP conjugate, reference serum, and goat IgG ELISA quantitation kit were obtained from Bethyl Laboratories (Montgomery, TX).

PEG Silane Modification and Photoresist Patterning on ITO Coated Glass Substrates. ITO coated glass slides were treated in an oxygen plasma chamber (YES-R3, San Jose, CA) at 300 W for 5 min. Afterward, the slides were incubated in 2% v/v 2-[methoxy(polyethylenoxy)propyl] trichlorosilane (PEG silane) dissolved in anhydrous toluene for 2 h. This reaction was performed in a glovebag under nitrogen purge to avoid atmospheric moisture. After PEG silane modification, the slides were rinsed in fresh toluene, dried under nitrogen, and cured at 100 °C for 2 h. Modified slides were then stored in a desiccator until further use.

Positive photoresist (AZ 5214-E) was spin-coated on PEG silane modified ITO substrate at 800 rpm for 10 s, followed by 4000 rpm for 30 s. The photoresist-coated slide was then soft-baked on a hot plate at 100 °C for 105 s. After baking, the photoresist layer (PR) was exposed to UV light (10 mW/cm^2) through a photomask for 45 s using a Canon PLA-501F Mask Aligner. Exposed photoresist was then developed for 5 min in AZ 300 MIF developer solution, briefly washed with DI water to remove residual developer solution, and then dried using nitrogen. The resultant photopatterned substrate was then hard baked for 30 min at 120 °C.

Characterization of PEG Silane Removal and Protein Deposition. A photopatterned substrate was exposed to oxygen plasma at 300W for 10 min to remove PEG silane from regions unprotected by photoresist. This resulted in formation of holes in the PEG silane monolayer. To deposit proteins in these holes, the substrate was incubated with 0.1 mg/mL collagen I in 1× PBS solution for 60 min, followed by a rinsing with DI water and drying under nitrogen. The substrate was then sonicated in acetone for 30 min to remove (lift-off) remaining photoresist from the surface leading to the formation of collagen domains surrounded by PEG silane on ITO.

Secondary ion mass spectrometry (SIMS) coupled with time-of-flight (ToF) spectrometer was used to verify the removal of PEG silane using oxygen plasma and the deposition of collagen on ITO. Effusion C_{60}^+ ions were accelerated to 16 keV and steered toward a negatively biased target (−10 keV) to create a total impact energy of 26 keV. The feature of this technique is running SIMS in the event-by-event bombardment/detection mode. The secondary ions generated from each single impact were detected by an eight-anode detector. Each single impact was detected and recorded as an individual event. As reported by us previously, the secondary ion emission hemispheric volume of a single projectile impact was determined to be 5−10 nm in diameter (33, 34). The accumulation of ~2×10^6 events constituted a conventional secondary ion mass spectrum. The secondary ion yield is the number of secondary ions emitted per projectile impact. The yield of a detected ion A is calculated using eq 1

$$Y_A = \sum_{x_A} \frac{x_A N(x_A)}{N_{total}} = \sum_{x_A} x_A P(x_A) = \frac{I_A}{N_{total}} \qquad (1)$$

where x_A is the number of detected ions A in a single event ($0 \le x_A < 8$), $N(x_A)$ is total number of events when ions A were detected, N_{total} is the total number of projectile impacts, $P(x_A)$ is the probability distribution of detecting ions A in a single event, and I_A is the measured number of events when ion A is detected.

Imaging ellipsometry (IE) was also used to characterize the topology of the substrate and further verify the removal of PEG silane and the deposition of collagen. For these experiments, collagen I patterns were created on PEG silane-modified ITO using photoresist lithography protocols detailed above. For comparison and ease of characterization, identical procedures were followed to produce patterns on silicon wafers. The measurements were taken using an iElli2000 imaging null ellipsometer (Nanofilm, Gottingen, Germany) with a 20 mW Nd:YAG frequency-doubled laser operating at 1% power. Spatial maps of the ellipsometric parameter, δ, were acquired using a 10× objective, giving a field of view of 645 × 430 μm and a lateral resolution of 2 μm. δ maps were acquired using a series of 70 images collected over 4° of polarizer rotation. The null conditions of each pixel were then determined from this series of images and used to calculate δ values. Topographical maps of thickness were generated from these δ values using an optical model that assumed isotropic parallel slabs and a refractive index of 1.47 for both the PEG silane and collagen whereas a refractive index of 2.0 + 0.0075i was used for ITO. Average values were calculated on four separate 25 × 25 pixel regions on collagen and silane to characterize the roughness of the organic layer.

In addition, atomic force microscopy (AFM) was used to verify the thickness changes during PEG silane removal and collagen adsorption. All surface scans employed a Dimension 3100 Scanning Probe Microscope with a Hybrid closed-loop XYZ head and Nanoscope IVa controller (Vecco, Santa Barbara, CA). All samples were imaged in air or under Millipore water with a direct drive cantilever holder for fluids (Vecco, Santa Barbara, CA). Samples were scanned at 0.5 Hz in contact mode with 512 points collected in each of 512 scan lines. A silicon nitride cantilever with a spring constant of 0.05 N/m was used. A third order flattening routine was used to correct for bowing of the piezo during sample scanning.

Micropatterning of Proteins and Cells on ITO Substrates. To demonstrate the ability to define protein attachment sites, the micropatterned ITO surfaces were incubated in collagen-FITC solution (0.1 mg/mL) for 30 min, washed in 1X PBS three times, and rinsed in DI water. The samples were dried under nitrogen and imaged using LSM 5 Pascal confocal microscope (Carl Zeiss).

ITO substrates containing protein micropatterns were also incubated with cells to demonstrate that cell attachment could be controlled in a spatially resolved fashion (see Figure 1, step 3). The cell types used in our studies were human hepatic cell line (HepG2), primary rat hepatocytes, and murine 3T3 fibroblasts. HepG2 cells were maintained in MEM supplemented with 10% FBS, 200 U/ml penicillin, 200 μg/mL streptomycin, 1 mM sodium pyruvate, 1 mM nonessential amino acids at 37 °C in a humidified 5% CO_2 atmosphere. Primary rat hepatocytes were isolated from adult female Lewis rats (Charles River Laboratories, Boston, MA) weighing 125−200 g, using a two-step collagenase perfusion procedure as described previously (35). Typically, 100−200 million hepatocytes were obtained with viability of >90% as determined by trypan blue exclusion. Primary hepatocytes were maintained in DMEM supplemented with epidermal growth factor, glucagon, hydrocortisone sodium succinate, recombinant human insulin, 200 units/mL penicillin, 200 μg/mL streptomycin, and 10% FBS. Murine 3T3 fibroblasts were maintained in DMEM supplemented with 10% FBS, 200 U/ml penicillin, 200 μg/mL streptomycin at 37 °C in a humidified 5% CO_2 atmosphere. Prior to cell seeding, an ITO substrate with collagen micropatterns was sterilized with 70% ethanol, washed twice with 1× PBS and placed into a well of a 6-well plate before being incubated with a 3 mL of cell suspension of hepatocytes in culture medium with 10% FBS at a concentra-

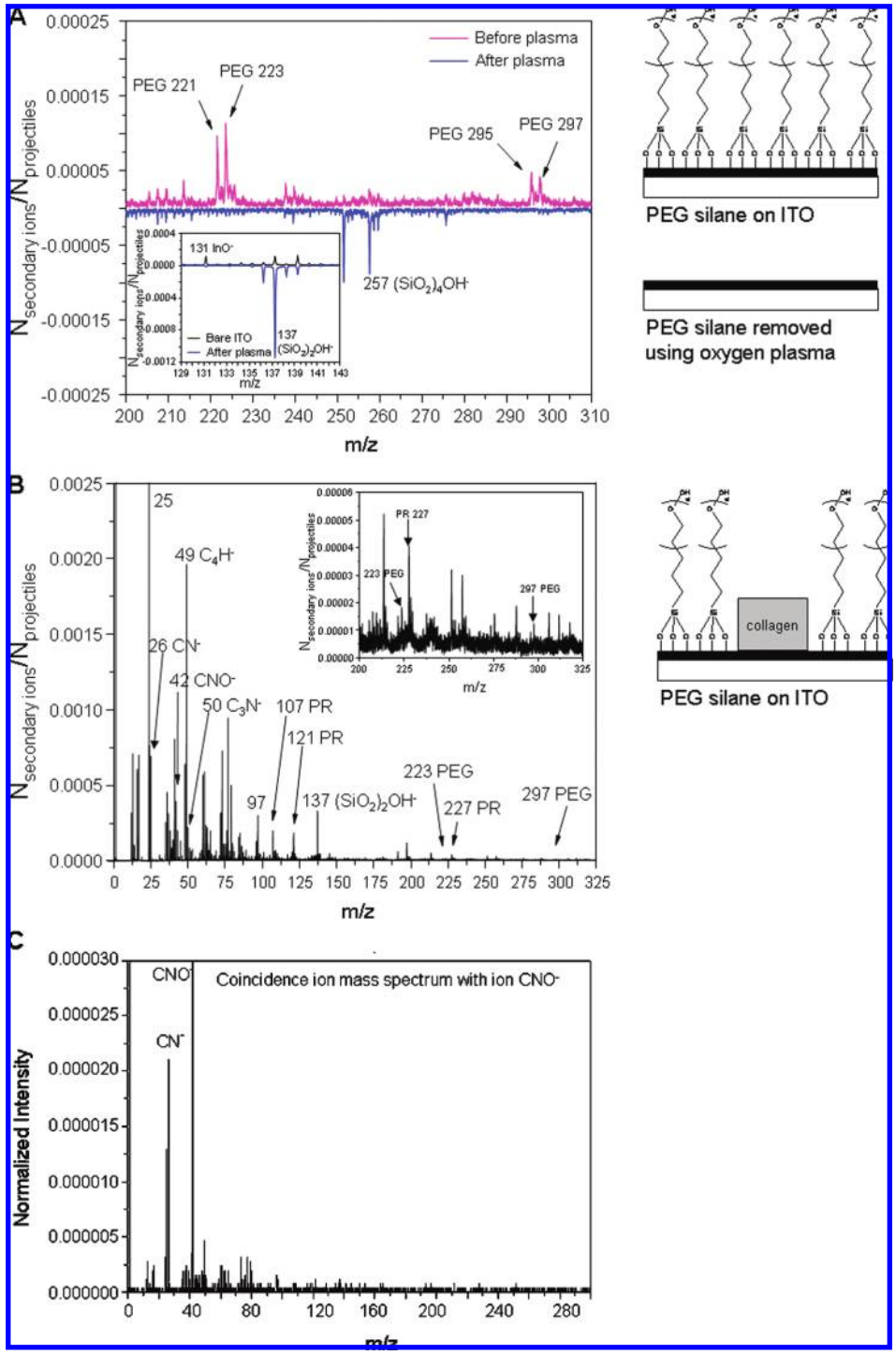

FIGURE 2. Characterization of PEG silane removal and protein micropatterns using ToF-SIMS. (A) The negative ion mass spectra of before and after oxygen plasma treatment shows disappearance of PEG peaks. (B) The negative ion mass spectra of 100 μm collagen micropatterns formed on PEG-modified ITO after removal of the photoresist (PR) layer. (C) Coincidence ion mass spectrum shows that emission of CNO^- ions (peptide bond components) is not associated with PEG or PR ion signatures. This suggests successful micropatterning of collagen.

tion of 1×10^6 cells/ml. After 1 h of incubation, unattached cells were aspirated and the medium replaced to leave behind patterned cellular arrays visualized using Zeiss Axiovert 40 microscope.

Electrochemical Desorption of PEG Silane Layer and Formation of Cocultures. The surface modification and cell seeding procedure described in the previous section resulted in cells attaching onto microdomains defined within a PEG silane layer (see Figure 1, step 3). To form cocultures, electrochemical desorption of the PEG layer was employed to make previously nonfouling regions of the ITO substrate conducive to cell adhesion. Electrochemical desorption of PEG silane self-assembled on ITO substrates was described by us previously (21). Briefly, an ITO substrate containing islands of hepatocytes (50 to 300 μm diameter) was placed into a custom-made Plexiglas electrochemical cell and immersed in 500 μL of cell culture media acting as an electrolyte solution. Ag/AgCl reference and Pt counter electrodes were positioned in the same electrochemical cell with ITO region serving as a working electrode and a steel wire providing electrical contact with the

Table 1. Yields of Negative Ions InO^- at $m/z = 131$ and PEG Fragments at $m/z = 223$ from Bare ITO, PEG Silane Modified ITO and PEG Silane Coated ITO Treated with Oxygen Plasma to Remove PEG from the Substrates

samples	Y_{InO^-} (m/z =131)	Y_{PEG} (m/z = 223)
1. Bare ITO	1.11×10^{-3}	*a*
2. PEG coating	2.60×10^{-4}	2.70×10^{-3}
3. after O_2 clean	1.95×10^{-4}	*a*

[a] Indicates absence of a peak.

substrate. Reductive potential of −1.4 V was applied for 60 s, followed by washing with fresh media. This procedure led to removal of the PEG silane layer surrounding the islands of hepatocytes and allowed to add another cell type, 3T3 fibroblasts, onto the same surface. Fibroblasts were incubated at a concentration of 0.5×10^6 cells/mL to create hepatocyte-fibroblast cocultures. Production of albumin by the hepatocytes was assessed using standard ELISA protocols to evaluate function of hepatocytes on ITO substrates (35).

RESULTS AND DISCUSSION

In this study, we present a novel approach that combines photolithography, oxygen plasma treatment and electrochemical switching of the biointerface to create micropatterned cocultures on ITO substrates (Figure 1). Different steps in this surface micropatterning procedure were characterized by ToF-SIMS, imaging ellipsometry and AFM. Micropatterning of cells and creation of functional hepatocyte-fibroblast cocultures on ITO substrates was also demonstrated pointing to future applications of this approach in cell cultivation, tissue engineering and biosensing.

Chemical Analysis of Micropatterned Surfaces Using ToF-SIMS. The goal of this study was to develop a simple and effective strategy for patterning two cell types on the same surface. A first step in creating this complex micropatterned substrate was to define cell-adhesive microdomains on a nonfouling, PEG-modified ITO substrate. We chose to employ a strategy described by Folch and coworkers whereby nonfouling substrates are covered with a stencil and then treated with oxygen plasma to remove nonfouling molecules from specific regions (36). In our approach, described in Figure 1, a photoresist pattern fabricated on PEG silane-modified ITO substrate served as a protective layer during the oxygen plasma exposure. Plasma treatment removed PEG molecules from regions of ITO substrates not protected by photoresist. This allowed for protein (collagen I) adsorption to occur within etched-out regions of the surface. Removal of the photoresist created an array of protein islands within a layer of PEG-silane (see Figure 1).

ToF-SIMS analysis was employed to characterize chemical composition at different stages in the construction of micropatterned surfaces. Unlike imaging ToF-SIMS that is used more commonly for micropattern characterization (37, 38), our surfaces were characterized by 26 keV C_{60}^+ ToF-SIMS running in the event-by-event bombardment-detection mode (34, 39). In this approach, surface is bombarded by projectiles (e.g., C_{60}^+ particles) and a single projectile impact creates a hemispherical "crater" of 5−10 nm in diameter (40). Mass spectra of each impact are detected one-at-a-time and are resolved in time and space. For example, using this method we could investigate ion masses coinciding with photoresist or PEG-silane signature peaks and could infer about contaminating chemical species present on the surface. Modification of ITO with PEG silane was confirmed by the presence of a silane related peak ($CH_3SiO_2^-$) at m/z = 75 (data not shown). The mass spectra of negative secondary ions emitted from surfaces of PEG silane-modified ITO before and after plasma ashing are shown in Figure 2A. The characteristic ion of PEG molecules is at $m/z = 223$ while the indium oxide ion (InO^-) is at $m/z = 131$. The yields of 131 and 223 secondary ions corresponding to ITO and PEG silane-modified ITO were calculated based on mass spectra obtained before and after oxygen plasma treatment. These data, presented in Table 1, point to complete removal of PEG molecules after exposure to oxygen plasma. In addition, absence of the silane peak ($m/z = 75$) after oxygen plasma treatment also indicated removal of silane molecules. It should also be noted that in addition to disappearance of PEG mass (223) oxygen plasma treatment also caused a decrease in the yield of $m/z = 131$ associated with InO^- ion of ITO and an increase in the yields of glass correlated peaks at $m/z = 137$ $(SiO_2)_2OH^-$ and $m/z = 257$ $(SiO_2)_4OH^-$ (Figure 2A and Table 1). This suggested etching or chemical modification of the outer layer of ITO. This did not impact our ability to culture cells on the surface; however, the oxygen plasma exposure may need to be optimized in the future to eliminate overetching. Given that the depth of penetration of C_{60}^+ ions used in surface bombardment was estimated to be ∼10 nm (40), appearance of secondary InO^- ions in mass spectra of PEG-modified ITO indicates that PEG silane thickness is less than 10 nm. Imaging ellipsometry and AFM data presented in the following section validate this observation.

ToF-SIMS analysis was also used to characterize deposition of the protein in regions exposed to oxygen plasma. For these experiments, photolithography was used to make 100 μm photoresist arrays on PEG silane-modified ITO substrates. Oxygen plasma was used to remove PEG silane from the exposed regions as described earlier. Following this, the surface was incubated with collagen and sonicated in acetone to dissolve remaining photoresist. After the lift-off process the collagen molecules adsorbed on ITO were expected to remain on the surface while protein molecules deposited on photoresist were expected to be removed. After photoresist removal, the surface was expected to contain collagen islands surrounded by the PEG-silane layer (see Figure 1 for description). SIMS analysis of this micropatterned surface (shown in Figure 2B) pointed to the presence of several ion fragments associated with peptide bonds (CN^-, CNO^-, and C_3N^-). The lift-off process led to a decrease in intensity of protein segments confirming the removal of collagen adsorbed on top of the resist. Importantly, protein fragments were colocalized in the same spectrum with fragments characteristic of PEG silane at

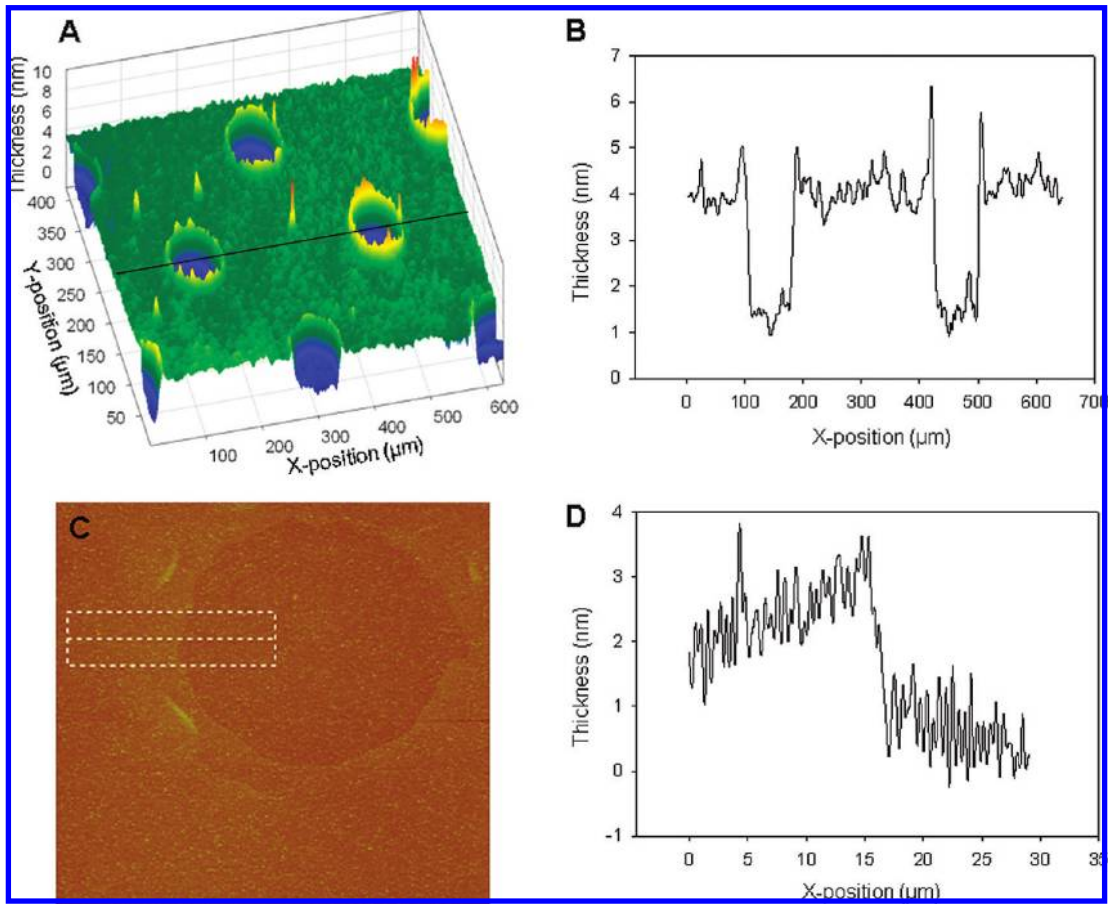

FIGURE 3. Imaging recesses etched out in PEG silane layer with oxygen plasma. (A) A topograph showing holes in PEG silane on ITO due to oxygen plasma ashing using imaging ellipsometry with (B) corresponding cursor profile. The depth of the holes is ~3 nm pointing to the complete removal of PEG silane. (C) AFM micrograph with (D) corresponding surface profile of holes on ITO shows agreement of the depth of holes.

m/z 223 ($C_9H_{19}O_6^-$) and 297 ($C_{12}H_{25}O_8^-$) confirming the presence of both regions on the surface. Interestingly, we also observed peaks at *m/z* 107 ($CH_2C_6H_4OH^-$) and 227 ($C_{15}H_{13}(OH)_2^-$) that could be associated with photoresist. This suggested that some photoresist residues remained on the surface after the lift-off process. Similar observation has been made before by Grainger and colleagues characterizing photolithography-based surface patterning technique (37, 38). While this is an important finding, we did not observe problems with attachment and function of cells due to photoresist contamination. This corroborates our previous finding that photoresist patterning and lift-off process (acetone exposure) had no detrimental effect on cell attachment and function (41).

To better understand the properties of cell adhesive regions, we also examined chemical composition of the micropatterned surface after modification with collagen (I). In this set of ToF-SIMS experiments we analyzed secondary ions coemitted alongside a signature protein fragment (CNO^-) (39). Our mass spectrometric analysis allowed to detect secondary ions emitted from each C_{60}^+ projectile striking the surface and provided direct evidence of the chemical composition of the 10 nm diameter crater created by the impact. The resulting coincidence ion mass spectrum (Figure 2C) shows a strong peak at *m/z* = 26 (CN^-) coemitted with the CNO^- and underscores the presence of protein (collagen) on the surface. At the same time we observed only low intensity signal of PEG and photoresist (PR) ions colocalized with peptide fragments, suggesting minimal contamination of collagen domains.

Imaging Micropatterned Surfaces with Ellipsometry and Atomic Force Microscopy. Imaging ellipsometry (IE) was employed to visualize the ITO surface after creating micropatterns in the PEG silane layer using oxygen plasma. Figure 3A shows a typical plot of the ellipsometrically determined optical thickness of plasma cleaned circular regions etched into the PEG silane layer. A corresponding line scan is shown in Figure 3B and denoted by the black line in panel A. The average depth of the observed features is 2.9 ± 0.4 nm, suggesting full removal of the PEG silane layer (21). Furthermore, the shape and dimensions of the holes (100 μm diameter) correspond with high fidelity to these openings of the photoresist pattern. Some thicker imperfections are visible at the edges of the etched out circular regions. These are likely a result of residual photoresist at the ITO - PEG silane interface. The optical thickness of these imperfections may be exaggerated as a result of refractive index differences not accounted for in the modeling of the data. Similarly, the nonzero thickness value of the well is likely an artifact of the variation in ITO thickness on the sample surface. The applied optical model

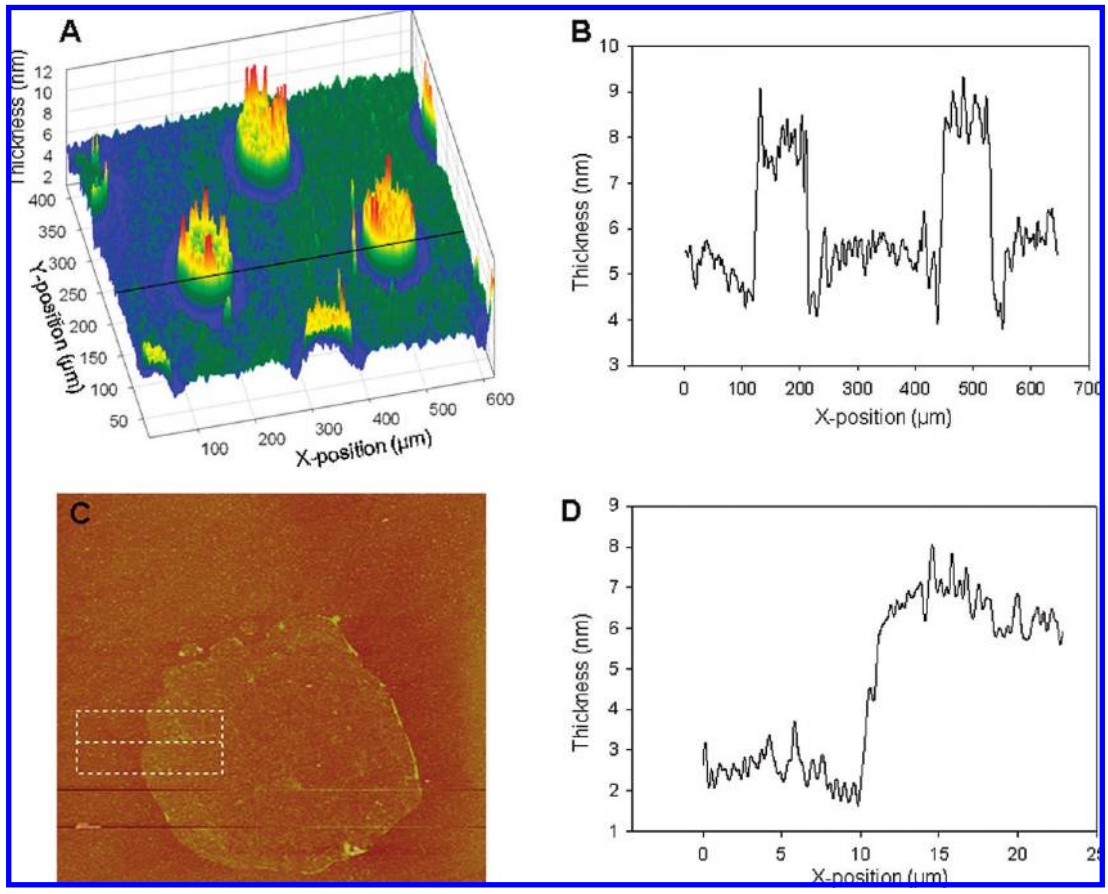

FIGURE 4. Imaging protein islands created by filling the recesses. (A) A topograph showing protein micropatterns on ITO using imaging ellipsometry with (B) corresponding cursor profile. (C) AFM micrograph and (D) corresponding surface profile of collagen pillars on ITO surrounded by PEG silane. The height of the collagen pillars from PEG silane calculated using imaging ellipsometer and AFM is ~3.5 nm.

assumes a 189 nm thick ITO layer, the average obtained from previous measurements of the sample. Local variations from this thickness will shift the baseline thickness accordingly.

AFM characterization of a similar sample confirms the excellent pattern fidelity and offers some insight into the finer structure of the features. A 90 × 90 μm AFM scan is shown in Figure 3C. The higher lateral resolution of AFM shows that the feature edge is not perfectly smooth and some deviations from the circle are observed. These deviations may result from defects within the mask or photoresist or possibly from undercutting during the plasma ashing process. A corresponding height profile is shown in Figure 3D. The profile was obtained by averaging the line scans within the white box shown in Figure 3C. Some uncorrected bowing of the piezo can be seen in the line scan as well. The observed step height is in good agreement with the optically determined thicknesses above, again confirming the full removal of the PEG silane layer. In the IE and AFM images, the granularity of the ITO layer is apparent in both the PEG silane and etched ITO regions. Using AFM we calculate the rms roughness to be 2.4 nm in both regions, showing that the etching process does not substantially change the physical surface characteristics.

After deposition of collagen, samples were again characterized using IE and AFM. Figure 4A shows a typical plot of the ellipsometrically determined optical thickness of a sample after collagen deposition with a corresponding line scan in Figure 4B. With the PEG silane regions, the ellipsometric parameters and corresponding thicknesses remain relatively unchanged from the values prior to collagen deposition. However a large increase in thickness is observed within the wells. This indicates that collagen has adsorbed selectively into the etched regions within the PEG silane layer. Across the sample, we measure an average thickness increase of 6.1 ± 0.6 nm within the etched regions. AFM characterization confirms the morphology of these features. An AFM scan and corresponding height profile are shown in Figure 4C and D. Again we observe excellent pattern fidelity and confirm the selective adsorption to the etched regions. We measure an rms roughness of 2.5 nm for the PEG silane regions and 3.0 for the collagen. Interestingly, we note that the height of the collagen in this feature is larger than that observed by IE. This larger step height may be a result of our choice of a model using a single refractive index for both PEG silane and collagen regions.

Micropatterning of Proteins and Cells on ITO Substrates. To demonstrate biological applications of our surface modification approach ITO substrates containing collagen micropatterns were incubated with mammalian cells. Figure 5A, shows FITC-conjugated collagen (I) patterns adsorbed onto ITO substrate through the photoresist stencil. The fact that protein deposition did occur points to the

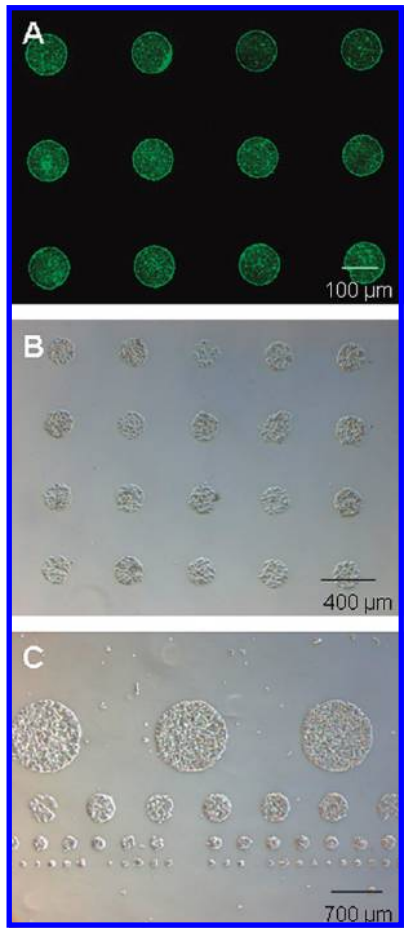

FIGURE 5. Selective adsorption of proteins and cells in the regions etched within PEG silane using oxygen plasma. (A) Selective adsorption of collagen-FITC ITO regions exposed to oxygen plasma. Note lack of protein deposition to surrounding ITO regions that remain nonfouling due to the presence of PEG silane. (B) Preferential attachment of hepatocytes to form cellular micropatterns on collagen-containing regions of ITO. The remainder of the ITO surface contained PEG silane and remained non-adhesive for cells. (C) Formation of cellular patterns ranging from 50 to 1000 μm in diameter.

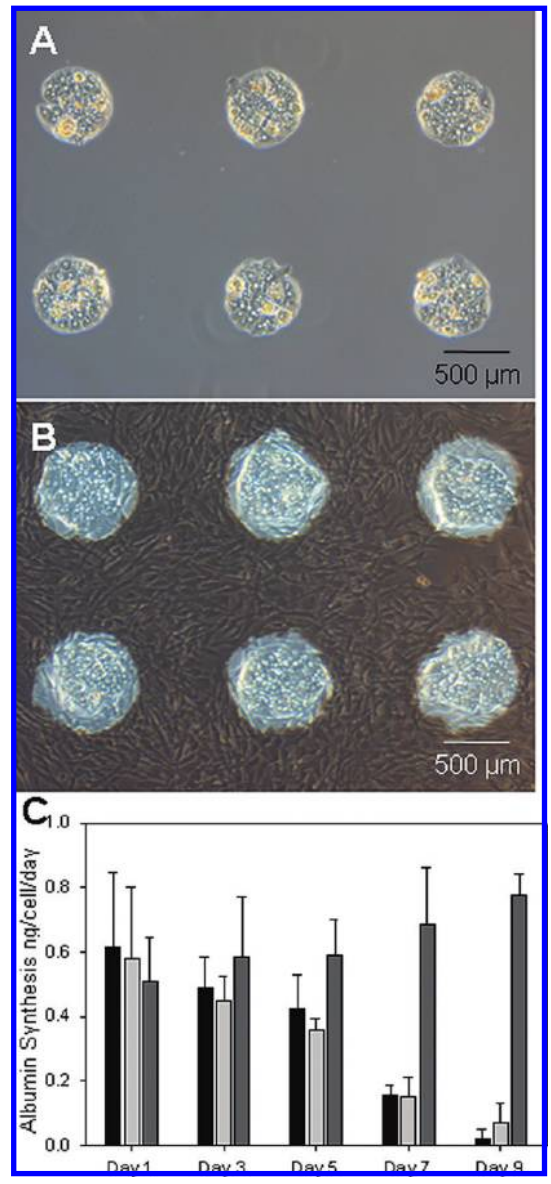

FIGURE 6. Assembly of a micropatterned cocultures on ITO substrates. (A) Primary rat hepatocytes attach on collagen islands defined within a nonfouling PEG silane layer. (B) Applying voltage (−1.4 V vs Ag/AgCl reference) leads to the desorption of PEG silane, switching ITO surface properties from nonfouling to cell-adhesive. A second cell type (3T3 fibroblasts) is seeded onto the surface containing hepatocytes. Micropatterned coculture is created. (C) ELISA analysis of albumin secretion by primary rat hepatocytes micropatterned in monocultures on glass (black), ITO (light gray), and in coculture with 3T3 fibroblasts on ITO (dark gray).

removal of the nonfouling PEG molecules during oxygen plasma treatment. Incubation of this surface with hepatic cells (Figure 5B, C) or fibroblasts (not shown here) resulted in selective attachment of cells onto protein microdomains. Minimal cell attachment on the PEG silane-modified regions of ITO was observed. Importantly, cells were seeded in serum-containing medium; this underscores again the nonfouling properties of the surface. Figure 5C demonstrates the formation of cellular micropatterns ranging from 50 to 1000 μm, highlighting the ability to define the size of the cell cluster using our micropatterning strategy. Localized attachment of other cell types such as hepatic stellate cells and 3T3 fibroblasts that do not require ECM proteins to attach to the surface was also demonstrated (data not shown).

Electrochemical Switching of ITO Substrate and Formation of Micropatterned Cocultures. Oxygen plasma treatment of the photoresist patterned, PEG-silane modified ITO surface created cell adhesive islands within the nonfouling background. As shown in Figure 5, the pattern of adherent cells replicated with high-fidelity the design of the photoresist template. However, addition of the second cell type onto the same surface and construction of the coculture required that the previously nonfouling PEG-containing background become cell adhesive. This was achieved by applying reductive potential (−1.4 V vs AgCl) to the ITO substrate containing micropatterns of cell type 1. As described by us previously (21), a layer of PEG silane may be removed from the ITO surface under these conditions, thus switching interfacial properties from nonfoulling to cell-adhesive. After seeding cell type 2, micropatterns of two distinct cell types could be assembled on the surface. Figure 6 (A, B) demonstrates our ability to create micropat-

terned cocultures of primary rat hepatocytes and 3T3 fibroblasts using this approach.

Interestingly, applying voltage to the ITO substrate containing hepatocyte micropatterns did not result in the detachment of these cells and only resulted in the removal of the silane layer. This may seem contradictory to the reports by us and others describing electrochemical detachment of cells from electrode surfaces (22, 23). However, in these previous studies cells were residing on a structured layer of either alkanethiol or silane and were desorbed by electrochemical disruption of this anchoring layer. In the strategy described here, cells are residing on collagen molecules that are adsorbed directly onto the ITO substrate. The protein deposition on ITO is likely the result of multiple types of secondary forces including electrostatic, hydrophobic and van der Waals interactions. Therefore, applying reductive potential is not sufficient to remove collagen molecules and cells for the surface.

Primary hepatocytes are used commonly as liver surrogates in toxicology screening and in bioartificial liver assist devices (43). These cells are notoriously difficult to maintain in vitro and therefore offer an excellent indicator of biocompatibility of the micropatterning strategy described here. The differentiated hepatic phenotype is commonly characterized by detection of secreted hallmark liver proteins such as albumin. ELISA was used to analyze albumin production by hepatocytes in mono- and cocultures created on glass and ITO surfaces. As seen in Figure 6C, the amounts of albumin secreted by hepatocytes cultured on ITO and glass substrates were comparable ($N = 3$, $p > 0.05$). A similar decline in albumin production occurred on the both surfaces and was expected given rapid dedifferentiation of hepatocytes. Multiple studies have shown that cocultivation with stromal or nonparenchymal liver cells rescues the hepatocytes and improves hepatic function (4, 8). Albumin release data shown in Figure 6C confirm this fact and demonstrate that hepatocytes cocultivated with fibroblasts on ITO substrates remained highly function after 9 days in culture. The studies described in Figure 6C are significant for several reasons. (1) These results show that fragile primary hepatocytes remain highly functional on ITO substrates, suggesting that this substrate is compatible with difficult-to-culture primary cells. (2) Electrochemical switching of the ITO surface containing primary hepatocytes did not kill or harm these cells since the hepatocytes cultured on glass and not exposed to applied voltage showed similar albumin production. (3) Photoresist patterning and oxygen treatment of the surface did not appear to have detrimental (cytotoxic) effects on primary rat hepatocytes and 3T3 fibroblasts.

CONCLUSIONS

The goal of this paper was to develop and characterize a novel method for forming cellular micropatterns on ITO. In our surface engineering strategy, ITO surfaces were modified with PEG silane layer then protected by a photoresist pattern that in turn served as a stencil during oxygen plasma treatment of the surface. Adsorption of proteins on the surface was followed by removal of the photoresist and created cell-adhesive protein domains interspersed with nonfouling PEG regions. Importantly, electrochemical stimulation of the underlying ITO could be used to desorb the remaining PEG-silane layer and make the remainder of the surface conducive to cell attachment. Extensive characterization of micropattern composition and topography was performed. Coincidence SIMS analysis was used to verify chemical composition of the distinct regions of the micropatterns. In addition, imaging ellipsometry and AFM were employed to further validate presence of collagen molecules within the oxygen-etched regions of the PEG silane layer. While the thickness of the protein regions (~6 nm) pointed to multilayer deposition of collagen molecules, fibril formation was not observed. The ability of this micropatterning strategy to confine cell attachment to defined surface domains was demonstrated with several cell types, including 3T3 fibroblasts, stellate cells (data not shown in the paper) and primary rat hepatocytes. Importantly, the use of ITO as a substrate allowed us to electrically stimulate the surface containing cellular micropatterns of cell type I, detach PEG molecules from the surrounding regions and then seed cell type II to complete the coculture. Electrochemical switching provided the temporal control of when to add the second type. In addition, unlike coculture strategies described previously by us and others (8, 43), the present approach is not dependent on the sequence of cell seeding and cell type-specific adhesion preferences.

While electrical manipulation of biological interface and control over cell-surface interactions has garnered a lot of attention recently (15, 16, 18, 23), majority of these studies have focused on controlling cell attachment on gold. Our study is one of the few to employ ITO substrates for surface micropatterning, electrochemical switching and cell cultivation. Unlike the strategy described by Voros and colleagues who demonstrated release of custom-made PEG-poly L-lysine from negatively charged ITO substrates (29, 30), our method employed chlorosilanes and likely involved cleavage of siloxane bonds formed on ITO (21). Commercial availability of silanes with a variety of functional groups opens wide-ranging possibilities for designing and switching surface chemistry of ITO. Beyond switching of surface properties, conductivity of ITO may be used in the future to make electrical measurements of cell growth and function in micropatterned cocultures.

Acknowledgment. The authors would like to thank Ms. Caroline Jones for isolation of rat primary hepatocytes and Ms. Katelyn Cahill-Thompson for assistance with ELISA experiments. We thank Prof. Louie's lab in the Department of Biomedical Engineering at UC Davis for the use of confocal microscope. We also thank Prof. Pan's lab in the Department of Biomedical Engineering at UC Davis assistance with electrical measurements. Financial support for this grant was provided in part by NIH grant (EB006519) awarded to A.R. The work by E.A.S., S.V. and L.J.C. was supported by the National Science Foundation (CHE-0750377). A.N.P. and M.C.D acknowledge support from DOE grant number DE-FG02-04ER46173. S.S.S. was supported by Grant Number T32-GM08799 from NIGMS-NIH.

REFERENCES AND NOTES

(1) Folch, A.; Toner, M. *Annu. Rev. Biomed. Eng.* **2000**, *2*, 227.
(2) El-Ali, J.; Sorger, P. K.; Jensen, K. F. *Nature* **2006**, *442*, 403–411.
(3) Khademhosseini, A.; Langer, R.; Borenstein, J.; Vacanti, J. P. *Proc. Natl. Acad. Sci. U.S.A.* **2006**, *103*, 2480–2487.
(4) Corlu, A.; Ilyin, G.; Cariou, S.; Lamy, I.; Loyer, P.; Guguen-Guillouzo, C. *Cell Biol. Toxicol.* **1997**, *13*, 235–242.
(5) Guguen-Guillouzo, C.; Clement, B.; Lescoat, G.; Glaise, D.; Guillouzo, A. *Dev. Biol.* **1984**, *105*, 211–220.
(6) Bhatia, S. N.; Balis, U. J.; Yarmush, M. L.; Toner, M. *J. Biomater. Sci., Polym. Ed.* **1998**, *9*, 1137–1160.
(7) Bhatia, S. N.; Balis, U. J.; Yarmush, M. L.; Toner, M. *Biotechnol. Prog.* **1998**, *14*, 378–387.
(8) Bhatia, S. N.; Yarmush, M. L.; Toner, M. *J. Biomed. Mater. Res.* **1997**, *34*, 189–199.
(9) Folch, A.; Toner, M. *Biotechnol. Prog.* **1998**, *14*, 388–392.
(10) Whitesides, G. M.; Ostuni, E.; Takayama, S.; Jiang, X.; Ingber, D. E. *Annu. Rev. Biomed. Eng.* **2001**, *3*, 335–373.
(11) Folch, A.; Jo, B.-H.; Hurtado, O.; Beebe, D. J.; Toner, M. *J. Biomed. Mater. Res.* **2000**, *52*, 346–353.
(12) Wright, D.; Rajalingam, B.; Selvarasah, S.; Dokmeci, M. R.; Khademhosseini, A. *Lab Chip* **2007**, *7*, 1272–1279.
(13) Khademhosseini, A.; Suh, K. Y.; Yang, J. M.; Eng, G.; Yeh, J.; Levenberg, S.; Langer, R. *Biomaterials* **2004**, *25*, 3583–3592.
(14) Yamato, M.; Konno, C.; Utsumi, M.; Kikuchi, A.; Okano, T. *Biomaterials* **2002**, *23*, 561–567.
(15) Yousaf, M. N.; Houseman, B. T.; Mrksich, M. *Proc. Natl. Acad. Sci. U.S.A.* **2001**, *98*, 5992–5996.
(16) Yeo, W. S.; Yousaf, M. N.; Mrksich, M. *J. Am. Chem. Soc.* **2003**, *125*, 14994–14995.
(17) Lahann, J.; Mitragotri, S.; Tran, T. N.; Kaido, H.; Sundaram, J.; Choi, I. S.; Hoffer, S.; Somorjai, G. A.; Langer, R. *Science* **2003**, *299*, 371–374.
(18) Jiang, X.; Ferrigno, R.; Mrksich, M.; Whitesides, G. M. *J. Am. Chem. Soc.* **2003**, *125*, 2366–2367.
(19) Yeo, W. S.; Mrksich, M. *Langmuir* **2006**, *22*, 10816–10820.
(20) Li, Y.; Yuan, B.; Ji, H.; Han, D.; Chen, S. Q.; Tian, F.; Jiang, X. Y. *Angew. Chem., Int. Ed.* **2007**, *46*, 1094–1096.
(21) Shah, S. S.; Lee, J. Y.; Verkhoturov, S.; Tuleuova, N.; Schweikert, E. A.; Revzin, A. *Lanmguir* **2008**, *24*, 6837–6844.
(22) Zhu, H.; Yan, J.; Revzin, A. *Colloids Surf., B* **2008**, *54*, 250–258.
(23) Inaba, R.; Khademhosseini, A.; Suzuki, H.; Fukuda, J. *Biomaterials* **2009**, *30*, 3573–3579.
(24) Tang, C. S.; Dusseiller, M.; Makohliso, S.; Heuschkel, M.; Sharma, S.; Keller, B.; Voros, J. *Anal. Chem.* **2006**, *78*, 711–717.
(25) McClary, K.; Ugarova, T.; Grainger, D. *J. Biomed. Mater. Res.* **2000**, *50*, 428–439.
(26) Gross, G. W.; Wen, W. Y.; Lin, J. W. *J. Neurosci. Met.* **1985**, *15*, 243–252.
(27) Bieberich, E.; Guiseppi-Elie, A. *Biosens. Bioelectron.* **2004**, *19*, 923–931.
(28) Moore, E.; Rawley, O.; Wood, T.; Galvin, P. *Sens. Actuators, B* **2009**, *139*, 187–193.
(29) Tang, C.; Feller, L.; Rossbach, P.; Keller, B.; Voros, J.; Tosatti, S.; Textor, M. *Surf. Sci.* **2006**, *600*, 1510–1517.
(30) Guillaume-Gentil, O.; Akiyama, Y.; Schuler, M.; Tang, C.; Textor, M.; Yamato, M.; Okano, T.; Voros, J. *Adv. Mater.* **2008**, *20*, 560–565.
(31) Pale-Grosdenmange, C.; Simon, E. S.; Prime, K. L.; Whitesides, G. M. *J. Am. Chem. Soc.* **1991**, *113*, 12–20.
(32) Jo, S.; Park, K. *Biomaterials* **2000**, *21*, 605–616.
(33) Li, Z.; Verkhoturov, S. V.; Locklear, J. E.; Schweikert, E. A. *Int. J. Mass Spectrom.* **2008**, *269*, 112–117.
(34) Rickman, R. D.; , V. S.; Hager, G. J.; Schweikert, E. A. *Int. J. Mass Spectrom.* **2005**, *245*, 48–52.
(35) Dunn, J. C. Y.; Yarmush, M. L.; Koebe, H. G.; Tompkins, R. G. *FASEB J.* **1989**, *3*, 174–179.
(36) Tourovskaia, A.; Barber, T.; Wickes, B. T.; Hirdes, D.; Grin, B.; Castner, D. G.; Healy, K. E.; Folch, A. *Langmuir* **2003**, *19*, 4754–4764.
(37) Takahashi, H.; Emoto, K.; Dubey, M.; Castner, D. G.; Grainger, D. W. *Adv. Funct. Mater.* **2008**, *18*, 2079–2088.
(38) Dubey, M.; Emoto, K.; Cheng, F.; Gamble, L. J.; Takahashi, H.; Grainger, D. W.; Castner, D. G. *Surf. Interface Anal.* **2009**, *41*, 645–652.
(39) Park, M. A.; Gibson, K. A.; Quinones, L.; Schweikert, E. A. *Science* **1990**, *248*, 988–990.
(40) Li, Z.; Verkhoturov, S. V.; Schweikert, E. A. *Anal. Chem.* **2006**, *78*, 7410–7416.
(41) Lee, J. Y.; Zimmer, C.; Liu, G. Y.; Revzin, A. *Langmuir* **2008**, *24*, 2232–2239.
(42) Allen, J. W.; Hassanein, T.; Bhatia, S. N. *Hepatology* **2001**, *34*, 447–455.
(43) Revzin, A.; Rajagopalan, P.; Tilles, A. W.; Berthiaume, F.; Yarmush, M. L.; Toner, M. *Langmuir* **2004**, *20*, 2999–3005.

AM900508M